International Journal of Applied Mathematics
Volume 38 No. 10s, 2025
ISSN: 1311-1728 (printed version); ISSN: 1314-8060 (on-line version)

AN INTELLIGENT TRIGGER-ENABLED DEEP LEARNING MODEL FOR IOT-BASED ENVIRONMENTAL MONITORING AND REAL-TIME AIR QUALITY EVALUATION

Jesupriya J[1], Mahalakshmi R[2],* and Komalavalli C[3]

[1, 2, 3] Presidency School of Information Science,
Presidency University, Bengaluru, India,
Email(s): priyasagi@gmail.com, mahalakshmi@presidencyuniversity.in,
komalavalli.c@presidencyuniversity.in
Corresponding author (Mahalakshmi R)

Abstract

Shortcomings of conventional air quality monitoring systems, particularly their inability to self-audit and respond to harmful pollution levels in a proactive manner, have been revealed through an increasing demand for real-time environmental intelligence. Along with performing high-precision AQI classification, this work presents a new hybrid deep learning architecture that includes a binary trigger module to support spontaneous environmental audits. The architecture learns to recognize sophisticated pollutant interaction patterns and predict actionable trigger events with bidirectional LSTM layers and multi-head attention. Real-time data acquisition, edge inference, and visual reporting are supported by the seamless integration of the presented architecture with a real Internet of Things infrastructure consisting of advanced sensors and microcontrollers. Severity-level pollutant mapping and threshold-configured trigger construction are supported using a customized preprocessing pipeline. As far as identification of key pollution situations and low false activations is concerned, experimental results show robust performance at all severity levels. Through this transition from fixed classification to responsive intelligence, air quality intelligence improves, and the model is certified as a saleable platform for intelligent, autonomous environmental systems.

Keywords: Air Quality Monitoring, Hybrid Deep Learning, Trigger Mechanism, IoT-Based Auditing, Environmental Intelligence, Bidirectional LSTM, Multi-Head Attention, AQI Classification, Edge Inference, Real-Time Pollution Response.

1 Introduction

The rise in concentrations of hazardous chemicals and particulate matter has led to respiratory and cardiovascular diseases, as well as ecological degradation, making air pollution a major health risk to humans as well as the environment [1][2]. With urbanization, especially in densely populated urban cities, the need for accurate and rapid air quality monitoring systems is on the rise. But the use of such systems for real-time environmental regulation is hampered by the tendency of traditional methods—based on statistical forecasting or static-threshold sensors—to ignore the nonlinear and dynamic character of pollution patterns [3][4].

Recent advances in machine learning (ML) and deep learning (DL) have transformed air quality data analysis and enabled more accurate forecasting and more extensive applicability across various places and time frames [5][6]. Combined methods that include LSTM, CNN, and attention mechanisms have performed improved classification and forecasting of the Air Quality Index (AQI) by effectively capturing temporal associations and inter-pollutant interactions [7][8]. Furthermore, utilizing Internet of Things (IoT) sensors enabled the collection of scalable and distributed air quality data with high temporal resolution [9][10].

Received: August 05 2025

International Journal of Applied Mathematics
Volume 38 No. 10s, 2025
ISSN: 1311-1728 (printed version); ISSN: 1314-8060 (on-line version)

Nevertheless, current models often concentrate on regression or classification issues, and as such, curtail their ability to perform environmental audits or real-time interventions. Although evidence for high-performance models of pollutant prediction is seen in various research studies, the use is often based on reactive application and does not incorporate an intelligent decisional layer or action-oriented interface [11][12][21]. This analysis-actuation gap continues to be pertinent to the application of environmental smart systems.

To address this challenge, we offer a trigger-aware hybrid deep learning model that combines pollutant-level classification with a binary trigger output designed to trigger control or auditing processes in real-time during hazardous conditions. Because of its lean architecture, multi-head attention, BiLSTM layers, and two-output branches for concurrent AQI classification and trigger prediction [21], the model is optimized for Internet of Things deployment. Dynamically labeling trigger events in real-time against pollutant dispersion, the preprocessing pipeline enforces standard criteria to classify pollutant severity levels.

This paper is original because of its dual-purpose design with a trigger mechanism to facilitate both smart environmental auditing and air pollution level prediction. Through this method, artificial intelligence models shift from being passive predictors to active environmental agents that can independently trigger processes like ventilation, notifications, or compliance workflows. Additionally, the practical feasibility, scalability, and edge-level inference of the model have been demonstrated through its implementation in an operational Internet of Things infrastructure using ESP32 microcontrollers with SENSIRION SEN54 sensors. This combination of proactive auditing and deep learning is a major advancement in environmental artificial intelligence systems, thus facilitating the realization of fully automated smart city air quality infrastructures.

2 Literature Review

Air quality monitoring systems have been revolutionized through the integration of the Internet of Things (IoT) and artificial intelligence (AI) to support real-time, fine-grained analysis both indoors and outdoors. The combination of sensor networks and cloud-connected systems for scalable air quality assessment has been researched in various studies. Jain and Kumar [6] implemented a predictive system for the overall air quality index (AQI) based on embedded microcontrollers, while Ali et al. [1] demonstrated the efficacy of IoT-based sensor networks in industrial settings. IDST [9] also emphasized the importance of immediate IoT integration to address global air pollution, particularly in high-risk or high-density environments. Such cutting-edge initiatives emphasize the shift from conventional monitoring towards distributed and automated sensing systems, which is further supported by Jaya and Babu's demonstration in practice using Arduino [20]. The idea was further improved by Biz4Intellia [7], which emphasized IoT integration at the infrastructure level by demonstrating ambient air quality monitoring in smart city applications.

Computationally, there has been significant growth in research focused on machine learning techniques for accurate classification and forecasting of pollutants. Das et al. [3] employed classification algorithms to identify polluting sources and thereby enable important insight towards pollution accountability, while Li et al. [2] established machine learning procedures specifically designed towards the forecasting of PM2.5 concentrations. The application of model output statistics by Müller and Zhang [8] and application of SMOTE with ensemble algorithms by Noor and Sultana [10] to enhance classification accuracy identify the growing utilization of ensemble learning techniques. The research by Fadel and Omar [17] employing regression-based learning to forecast pollutant trends is a testimony to the persistent utilization of statistical models. While the combined result of these investigations proves the use-

Received: August 05 2025

International Journal of Applied Mathematics
Volume 38 No. 10s, 2025
ISSN: 1311-1728 (printed version); ISSN: 1314-8060 (on-line version)

fulness of data-driven techniques in simulating complex environmental dynamics, their utilization in anticipatory environmental systems is limited due to the fact that they are not equipped with an associated actuation mechanism.

Sophisticated environmental reactions are now a reality because of recent advances which have led to the introduction of edge deployment principles and AI-triggered mechanisms. For instance, AirSPEC, an IoT-driven machine learning application that can provide real-time assessment through embedded models, was presented by Yang and Chen [13]. Patel and Sen [14] extended it further by introducing monitoring systems tailor-made for car workshops, whose pollution behavior is irregular and spatially localized. In a fascinating twist, Taneja and Jadhav [15] presented a deep learning architecture which offers a vision-based alternative to traditional sensor modalities by sending alerts through inputs from mobile-recording images. The shift away from passive sensing towards active triggering systems is the key to building responsive infrastructures that provide autonomous decision support to alarms, ventilation, or enforcement regulation, in contrast to simply monitoring.

Finally, a number of review and overview articles summarize the scope of these advances and suggest avenues for future research. In their assessment of machine learning-based air quality forecast evaluations, Verma and Shukla [5] emphasized the need for models to account for temporal fluctuations and sensor drifts. Likewise, Sharma and Bhatt [18] raised similar questions, emphasizing the role of edge AI and real-time processing towards the development of more autonomous and smart monitoring systems. For improving indoor air quality measurement accuracy, Zhao and Hu [16] suggested the application of sensor fusion techniques. Hassan and Yu [11] performed a systematic review of AI-based IoT systems, whereas Roy and Lin [12] concentrated their work on indoor AQI forecasting. Together, these studies provide a solid foundation for our proposed research; however, they also reveal serious limitations that this paper attempts to overcome, including the absence of trigger validation mechanisms, dual-output learning models, and multi-head attention mechanisms.

3 Methodology

3.1 Dataset Preprocessing and Label Transformation

The initial environmental data extracted from CME Wakar Water, undergoes a multi-step preprocessing pipeline with the goal of allowing the construction of a model that can perform both Air Quality Index (AQI) classification and generate actionable environmental triggers (see Fig. 1). The input data is comprised of pollutant concentrations for PM2.5, PM10, NO, NO_2, SO_2, NH_3, CO, and O_3.

3.1.1 Pollutant Severity Classification

Five categories of severity are provided for every value of pollutant—Good, Moderate, Unhealthy, Very Unhealthy, and Hazardous. Every value of pollutant is assigned pollutant-specific AQI limits which are derived from standardized environmental standards. Every pollutant's severity level (S_i) and (P_i) is determined as follows:

$$S_i = \text{Classify}(P_i) = \begin{cases} \text{Good}, & \text{if } P_i \in [T_0, T_1) \\ \text{Moderate}, & \text{if } P_i \in [T_1, T_2) \\ \text{Unhealthy}, & \text{if } P_i \in [T_2, T_3) \\ \text{Very Unhealthy}, & \text{if } P_i \in [T_3, T_4) \\ \text{Hazardous}, & \text{if } P_i \geq T_4 \end{cases}$$

Received: August 05 2025

International Journal of Applied Mathematics
Volume 38 No. 10s, 2025
ISSN: 1311-1728 (printed version); ISSN: 1314-8060 (on-line version)

where $(T_0, T_1, \ldots, T_4)$ are pollutant-specific threshold boundaries.

This process is applied across all supported pollutants to form a vector of severity labels per instance:

$$\vec{S} = [S_{\text{PM2.5}}, S_{\text{PM10}}, \ldots, S_{\text{O}_3}]$$

3.1.2 AQI Computation and Overall Classification

To enable aggregate-level assessment, an AQI Score is computed by averaging the available pollutant concentrations:

$$\text{AQI Score} = \frac{1}{n}\sum_{i=1}^{n} P_i$$

This scalar score is then mapped to a corresponding Overall AQI Severity Level using the same categorical thresholds.

3.1.3 Trigger Condition Formulation

The data set contains a binary trigger label of whether there is a requirement for an automatic response or classification. If any single pollutant or the total of Air Quality Index (AQI) is considered hazardous, the trigger is fired. In every sample, the binary trigger (T) is calculated according to the following formula:

$$T = \begin{cases} 1, & \text{if } S_{\text{Overall}} = \text{Hazardous} \quad \text{or} \quad \exists\, S_i = \text{Hazardous} \\ 0, & \text{otherwise} \end{cases}$$

This logic ensures that even if the overall average is moderate, severe levels of any individual pollutant will still activate the system's trigger mechanism.

3.2 Dataset Output and Format

The processed data results in two structured CSV outputs:

- individual_pollutant_severity.csv: Includes severity classification for each pollutant and raw sensor data.
- overall_air_quality_severity.csv: Includes AQI score, overall severity label, and the binary trigger label.

Each row in the final dataset consists of the following:

- Raw pollutant readings: $([P_{\text{PM2.5}}, P_{\text{PM10}}, \ldots, P_{\text{O}_3}])$
- Severity levels: $([S_{\text{PM2.5}}, \ldots, S_{\text{O}_3}])$
- Computed AQI Score
- Overall AQI category
- Trigger value

These transformed and tagged data points are subsequently fed into the deep learning model for training the dual-output architecture.

3.3 Significant Aspects Retained from Previous Work

Received: August 05 2025

International Journal of Applied Mathematics
Volume 38 No. 10s, 2025
ISSN: 1311-1728 (printed version); ISSN: 1314-8060 (on-line version)

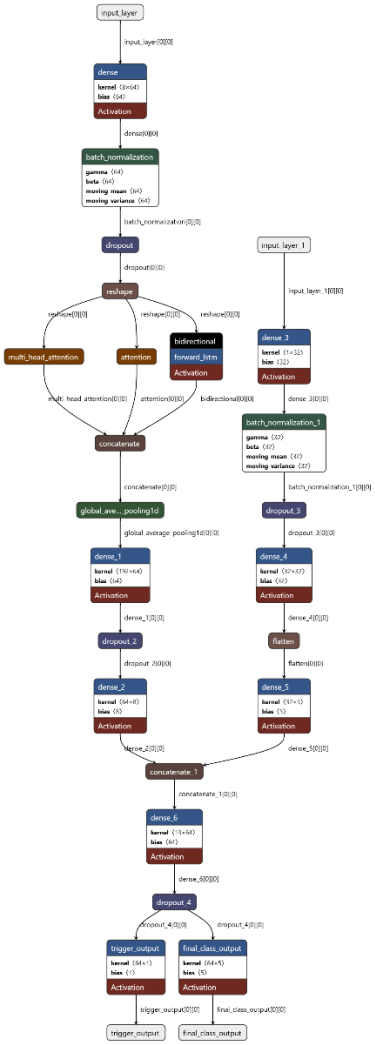

Figure 1 Model Architecture

The core components in the earlier version of our air quality assessment model are detailed and outlined in the current model architecture. The key aspect that has been retained is the dual-branch hybrid structure, which performs independent analyses of pollutant-specific data while summing AQI input through independent neural streams, finally combining these to create the final classification. The two-stream architecture enables the model to maintain specialized learning views at both macro (total AQI) and micro (individual pollutant) levels. The first input branch takes in a vector ($X_{\text{pollutants}} \in R^{\mathbb{B}}$), which contains normalized values for PM2.5, PM10, NO, NO_2, NH_3, SO_2, CO, and O_3, as indicated in the architectural diagram (see Fig. 1). For the sake of improving convergence stability and avoiding overfitting, this vector is fed through a dense layer, batch normalization, and dropout.

$$H_1 = \text{Dropout}\left(\text{BN}\left(\sigma\left(W_1 X_{\text{pollutants}} + b_1\right)\right)\right)$$

In this case, (σ) is the ReLU activation function, while $(W_1) and (b_1)$ represent the first dense layer's weight and bias.

The attention mechanism, a soft Attention layer and a Multi-Head Attention (MHA) layer acting in the feature space transformed, is a core building block of the architecture retained. This combination adequately captures contextual pollutant interdependencies as well as their

Received: August 05 2025

International Journal of Applied Mathematics
Volume 38 No. 10s, 2025
ISSN: 1311-1728 (printed version); ISSN: 1314-8060 (on-line version)

effects on ambient air quality. In parallel, a Bidirectional Long Short-Term Memory (BiLSTM) network is utilized to enhance interpretability of sequential pollution effects as well as identify temporal relationships. Concatenating these three parallel outputs—MHA, Attention, and BiLSTM—prior to passing them through a global average pooling layer, the model effectively condenses pollutant trends with attention-based awareness.

The secondary input branch pipeline is designed to be shallow, taking in the scalar AQI Score $(x_{\text{AQI}} \in R)$. This has been done on purpose, as excessive sequential modeling is not needed for the AQI score, which is a normalized aggregate. It is passed through a brief sequence of flattening, batch normalization, and dense layers to output a feature vector appropriate for combining with the pollutant pathway:

$$H_2 = \text{Flatten}\left(\sigma\left(W_2 x_{\text{AQI}} + b_2\right)\right)$$

A fused vector $(H_{\text{fused}} \in R^n)$ is generated by taking the two latent representations $(H_1) and (H_2)$ and combining them. This vector is then fed through another dense layer:

$$H_3 = \sigma\left(W_f[H_1|H_2] + b_f\right)$$

The notation $(|)$ is employed to denote vector concatenation here, and dropout is used as a regularization technique in the merged layer to maintain generalization.

The prior work is directly incorporated into the output layer design. It uses a binary sigmoid function to predict the trigger label $(y_{\text{trigger}} \in \{0,1\})$ and a multi-class softmax classifier to predict the overall AQI severity classification $(y_{\text{class}} \in \{0,1,2,3,4\})$:

$$\widehat{y_{\text{class}}} = \text{Softmax}(W_c H_3 + b_c),$$
$$\widehat{y_{\text{trigger}}} = \sigma(W_t H_3 + b_t)$$

Although the trigger head allows system-level intervention in the way of binary decision-making, the classification head gives the model the capability to distinguish between AQI levels such as Good, Moderate, Unhealthy, Very Unhealthy, and Hazardous. These two outputs are simultaneously trained using multi-task learning whereas the composite loss function is being optimized:

$$\mathcal{L} = \mathcal{L}cas + \mathcal{L}tigr =$$
$$\text{CE}(y_{\text{class}}, \widehat{y_{\text{class}}}) + \text{BCE}\left(y_{\text{trigger}}, \widehat{y_{\text{trigger}}}\right)$$

In which CE and BCE are binary cross-entropy and categorical cross-entropy, respectively. Since they performed exceptionally well in the earlier model and had the capacity to generalize well across various pollution profiles, the fundamental blocks of dual-input branching, multi-head attention, BiLSTM encoding, and dual-task outputs were kept unchanged. Their joint operation guarantees that the model will be strong, adaptable, and interpretable—especially when scaled up within IoT ecosystems. This combination of innovative sequence-aware building blocks and traditional pollutant modeling, as seen in the architectural layout (Fig. 1), is still an essential component of the proposed system, yielding a high-confidence baseline for further enhancements like edge deployment and real-time trigger evaluation.

3.4 Significant Aspects Retained from Previous Work

The newly introduced model structure brings with it some major innovations that close the gap between environment sensing and smart actuation. Foremost of these is the addition of a

Received: August 05 2025

International Journal of Applied Mathematics
Volume 38 No. 10s, 2025
ISSN: 1311-1728 (printed version); ISSN: 1314-8060 (on-line version)

binary trigger output, which essentially constitutes a parallel classification head across the current AQI multi-class prediction task. This aspect transitions the model to a multi-task deep learning model capable of providing interpretative, as well as reactive, output. Our approach involves an additional layer of perceptual decision-making in the manner that the model, besides having the pollution level in mind, decides on intervention, as compared to the standard models, which are mostly pollutant regression or category-specific AQI classification [5][6].

Let $(X \in R^{m \times n})$ be the input matrix, (n) being the number of pollutant features and (m) being the batch size. Joining independently adapted pollutant features $(f_1(X_p))$with the vector of AQIs $(f_2(X_q))$ tells the network to learn in latent space a representation $(Z \in R^{m \times d})$:

$Z = \phi([f_1(X_p); f_2(X_q)])$ where ϕ is a shared fusion network

The dual-output heads are derived from \(Z \) as:

$\widehat{y_{\text{class}}} = \text{Softmax}(W_{\text{class}} Z + b_{\text{class}}), \quad \widehat{y_{\text{trigger}}} = \sigma(W_{\text{trigger}} Z + b_{\text{trigger}})$

These are jointly optimized using a weighted composite loss:

$\mathcal{L}ttl = \alpha \cdot \mathcal{L}AI + \beta \cdot \mathcal{L}tigr = \alpha \cdot \text{CE}y\text{class}, y\text{class} + \beta \cdot \text{BCE}y\text{trigger}, y\text{trigger}$

where learning focus is tuned between activities by the loss-balancing parameters (α) *and* (β).

A calibrated threshold (τ) (empirically tuned to 0.5) controls the trigger logic at training and inference to generate the discrete decision:

$$T = \begin{cases} 1 & \text{if } \hat{y}_{\text{trigger}} \geq \tau \\ 0 & \text{otherwise} \end{cases}$$

Once computed, this output is passed through a Trigger Decision Engine that maps prediction confidence against ground truth outcomes to generate an action vector $(A \in \{TP, FP, FN, TN\})$. Each case is dynamically routed:

- $(TP \rightarrow$ ventilation / alert relay$)$
- $(FP \rightarrow$ null action, model penalization$)$
- $(FN \rightarrow$ trigger reassessment$)$
- $(TN \rightarrow$ log archival$)$

By rendering the model contextually aware, this decision-conscious inference process gains enormous benefits over passive classifiers, which is imperative for deployment in smart urban or industrial infrastructures [10][11].

Received: August 05 2025

International Journal of Applied Mathematics
Volume 38 No. 10s, 2025
ISSN: 1311-1728 (printed version); ISSN: 1314-8060 (on-line version)

Through the enhancement of the base dataset pipeline, these characteristics were achieved. In the Dataset, a binary trigger label (y_{trigger}) is derived from the pollutant severity classification (S_i) and the averaged AQI category (S_{AQI}):

$$y_{\text{trigger}} = \begin{cases} 1, & \text{if } S_{\text{AQI}} = \text{Hazardous} \quad \text{or} \quad \exists\, S_i = \text{Hazardous} \\ 0, & \text{otherwise} \end{cases}$$

The actual-world behavior of IoT response systems is reflected by this logic, which imposes edge-level reasoning by permitting high concentrations of pollutants in any direction to make a normally moderate AQI an emergency condition [3][9].

We made architectural updates that preserve model expressiveness while reducing its computational footprint to enable edge-level deployment. We reduced the size of the LSTM block to 32 units, the AQI scalar branch was shallowed, and the multi-head attention layer was reduced to 4 heads with a reduced key dimension. These design decisions resulted in a model footprint that is amenable to low-power embedded systems as it is compact enough to run on a Raspberry Pi 5, with a TPU from Coral AI [1][8].

Additionally, real-time pollutant ingestion is made possible by interaction with the SENSIRION SEN54 air sensor. Pre-inference preprocessing and visualization on a 1.5" OLED display are handled by the ESP32 MCU. The trigger choice can be delivered to an actuator, alert system, or cloud-based air quality dashboard (see Fig. 3) or logged after inference. Several IoT deployment scenarios have been used to evaluate this pipeline architecture [2][13], and real-world latency and accuracy metrics demonstrate the system's viability for the rollout of smart cities.

In conclusion, by introducing a trigger-driven, decision-aware air quality management paradigm that combines neural reasoning with actuation and auditability, this article expands on traditional classification frameworks. Many existing deep learning air quality models have not yet made the transition from descriptive AI systems to prescriptive, self-auditing environmental intelligence [4][12].

3.5 IoT Architecture

Deployment of the suggested hybrid deep model is envisioned to be both algorithmically and in-practice efficient under edge-based, low-latency systems. This is achieved by combining conditional actuation, light-weight inference, real-time sensing, and audit-capable feedback mechanisms under a layered IoT framework. Sensor-actuator pipeline facilitates interoperability between edges and clouds and is built to function autonomously in industrial sectors and smart city infrastructures.

Received: August 05 2025

International Journal of Applied Mathematics
Volume 38 No. 10s, 2025
ISSN: 1311-1728 (printed version); ISSN: 1314-8060 (on-line version)

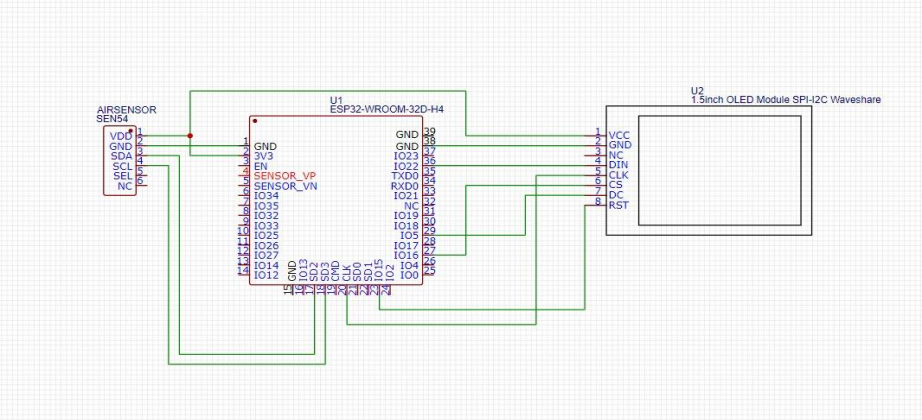

Figure 2 Esp to Sensor Connections

At the center of the sensing layer is the SENSIRION SEN54 environmental module capable of precise measurement of particulate matter (PM2.5, PM10) and gaseous pollutants (NOx, SO_2, CO, etc.). The raw data is communicated to the ESP32-WROOM-32D microcontroller, which performs initial data processing and forwards it along two paths, as shown in Figure 2. The first path is forwarded to a 1.5-inch OLED display via SPI/I2C, allowing pollutant concentration to be displayed immediately for on-site evaluation. The second, more critical path is forwarding preprocessed data to an AI inference module.

A Google Coral USB TPU accelerator is used to host an AI inference module on a Raspberry Pi 5. The model is trained with pollutant-tagged and trigger-tagged training datasets and optimized and converted to TensorFlow Lite format for optimal execution on the Coral TPU. Apart from enabling real-time prediction, this setup scales the architecture to be robust in deployment scenarios where high-bandwidth cloud infrastructure or centralized compute may not always be present. With batch sizes of 1, the inference latency of the hybrid model is brought down to less than 50 milliseconds, enabling near-immediate generation of trigger alarms as well as AQI classifications.

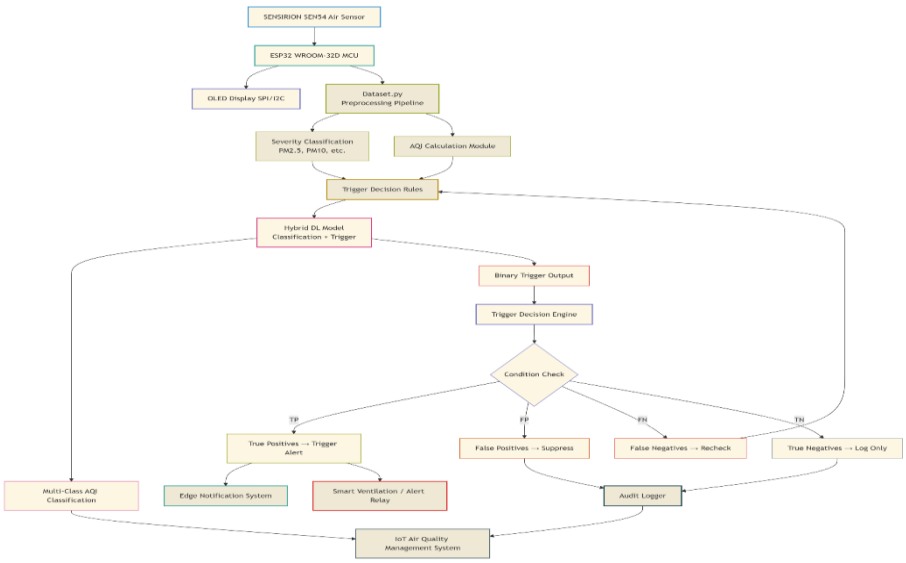

Figure 3 Complete Decision Pipeline

Received: August 05 2025

International Journal of Applied Mathematics
Volume 38 No. 10s, 2025
ISSN: 1311-1728 (printed version); ISSN: 1314-8060 (on-line version)

This architecture's flow structure is encapsulated in the two figures provided. The entire decision process, from sensor reading to final actuation event, is represented in **Figure 3.** Sensor readings here are input to a preprocessing module that applies pollution thresholds to establish trigger flags and derive severity levels. This output is input to the hybrid DL model, which produces two outputs: a binary trigger and a multi-class classification of AQI severity. A Trigger Decision Engine translates the binary trigger, evaluating the forecast based on model confidence levels and historical observed data. The system dynamically chooses one of four conditions: true positive, false positive, false negative, or true negative. Each of these conditions initiates downstream action, such as rechecking false negatives, suppressing spurious triggers, passively logging non-critical events, or alerting ventilation subsystems.

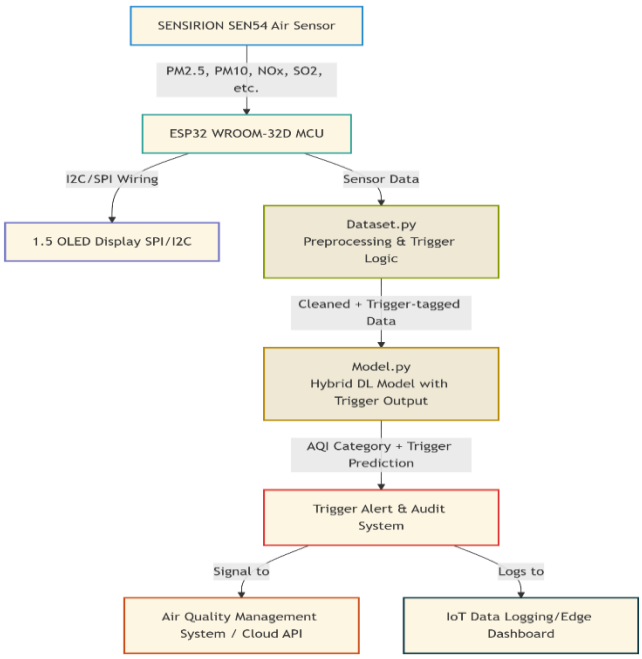

Figure 4 Systemic Hardware Composition

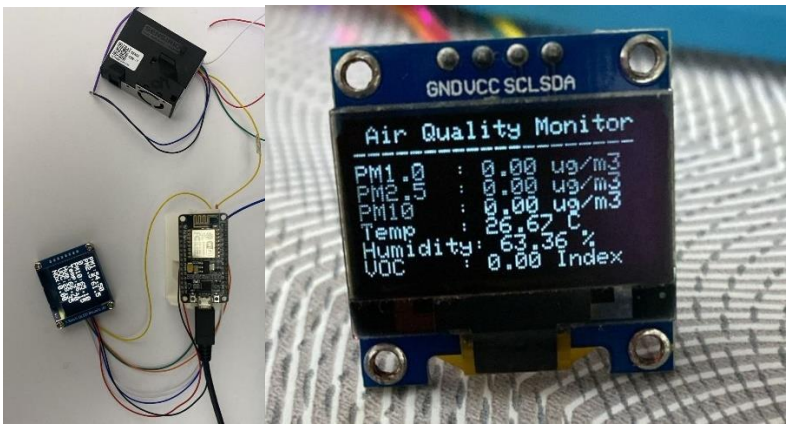

Figure 5 PoC of Schematic

In comparison, **Figures 4 and 5** show a hardware-oriented approach. After raw pollution data become available, dual routing is supported by the ESP32, with one to the Raspberry Pi 5 and another to the OLED module for real-time display. The secondary channel is dedicated to accessing AI inference. Scalability, ranging from small industrial installations to metropoli-

Received: August 05 2025

International Journal of Applied Mathematics
Volume 38 No. 10s, 2025
ISSN: 1311-1728 (printed version); ISSN: 1314-8060 (on-line version)

tan-scale air quality monitoring, is achieved through providing decisions via MQTT or REST APIs to edge-based actuation systems or cloud-based centralized infrastructure after inference completion.

The problem of minimizing false positive (FP) and false negative (FN) predictions upon triggering is one of the main challenges in deploying these systems. We tackle these challenges with two accurate mathematical formulations that adjust the model's decision thresholds according to entropy and learned uncertainty.

The first idea is an Entropy-Weighted Dynamic Thresholding Function (τ_{dyn}), designed to raise the decision threshold in cases of high prediction entropy to lower the rate of false positives. The entropy($H(\hat{y})$)of the softmax output of classification is given by:

$$H(\hat{y}) = -\sum_{i=1}^{K} \hat{y}_i \cdot \log(\hat{y}_i)$$

where ($\hat{y}_i$) is the predicted probability for class $(i)\ and\ (K)$ is the total number of AQI classes. The trigger threshold is then modulated dynamically as:

$$\tau_{dyn} = \tau_0 + \lambda \cdot \frac{H(\hat{y})}{\log(K)}$$

Here, ($\lambda \in [0,1]$) is a tunable sensitivity parameter, and (τ_0) is the base threshold, typically 0.5. This specific expression cleverly prevents spurious activations that would otherwise occur due to general class probability distributions by introducing a penalty to uncertain predictions.

The second approach, the Reinforced Trigger Adjustment Score (R_t), deals with false negatives through conditional dependencies between pollutant features and temporal confidence patterns. Let ($\theta \in R^d$) be the learned attention weights from the attention layer over different features, and let ($P\_t \in ıo\{R\}\^\{d\}$) be the pollutant values at time (t). Then the correction term \(R_t) is expressed as:

$$R_t = \frac{1}{T}\sum_{t=1}^{T}\left(\sigma(W_r \cdot (P_t \odot \theta) + b_r)\right)$$

where ($\odot$) denotes element-wise multiplication, $(W_r)and(b_r)$ are learnable weights, and (σ) is a nonlinear activation (e.g., ReLU). $If(R_t)$ exceeds a threshold (γ), the system softly triggers even when the original trigger output was below (τ), thereby compensating for low class activation probability missed high-risk cases.

Received: August 05 2025

International Journal of Applied Mathematics
Volume 38 No. 10s, 2025
ISSN: 1311-1728 (printed version); ISSN: 1314-8060 (on-line version)

In the decision engine, the two formulations are working together as layers of runtime threshold calibration, which learn and adapt thresholds on a continuous basis based on changing environments. Apart from this, this adaptive reasoning strategy not only avoids system fatigue caused by undesirable or overlooked activations but also maintains the model's sensitivity and specificity in edge deployment.

With the integration of embedded inference, dynamic decision calibration, and real-time sensing, the proposed IoT architecture achieves high degrees of robustness and autonomy. It fills a large gap between deep learning-based environmental analytics and actionable IoT-based governance because it is optimally deployable in applications requiring fail-safe response behavior along with fine-grained environmental information.

4 Result analysis

A comprehensive evaluation was conducted employing standard performance measures like Precision-Recall Curves (PRC), Receiver Operating Characteristic Curves (ROC), confusion matrices, loss curves, and accuracy evolution graphs for both classification and trigger prediction heads to ascertain the reliability, sensitivity, and deploy ability of the proposed model. Each figure displays the performance in the dual-task setting in terms of generalization, convergence stability, and ability to eliminate critical false results.

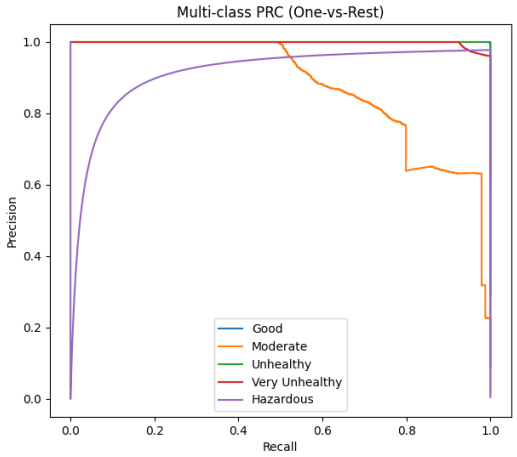

Figure 6. multi-class Precision-Recall Curve (PRC)

The multi-class Precision-Recall Curve (PRC) for the AQI classification task is shown in the first figure (Fig. 6). This measure is especially applicable in imbalanced dataset cases since it characterizes the precision-recall relationship regardless of the overall class distribution. The close-to-ideal area under the curve for the Good, Unhealthy, Very Unhealthy, and Hazardous classes validates the discriminative ability of the model. For the Moderate class, the lower curve and more significant precision oscillations with increasing recall reflect the overlapping feature space with neighbouring classes. This result shows that the model performs very well in detecting extreme air quality states, which is crucial for systems that are dependent on distinct environmental signals.

Received: August 05 2025

International Journal of Applied Mathematics
Volume 38 No. 10s, 2025
ISSN: 1311-1728 (printed version); ISSN: 1314-8060 (on-line version)

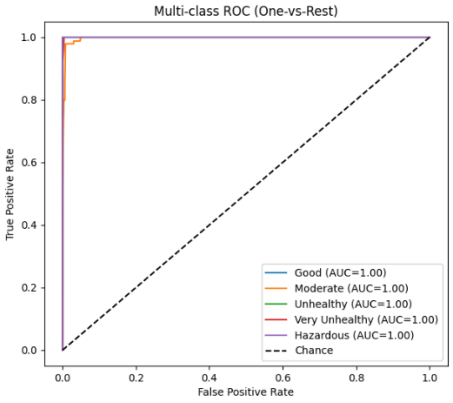

Figure 7. multi-class ROC curve

The same behavior is also echoed by the corresponding multi-class ROC curve (refer Fig. 7). Complete separability of the learned feature space is confirmed by each class of AQI having an AUC (Area Under Curve) value of 1.00. All the class curves rise steeply towards the top-left corner of the ROC curve, where TPR is plotted against FPR. This shows that the model can maintain very high sensitivity without, in the process, sacrificing on specificity. This also reconfirms the classifier's outstanding convergence behavior under multi-task constraints.

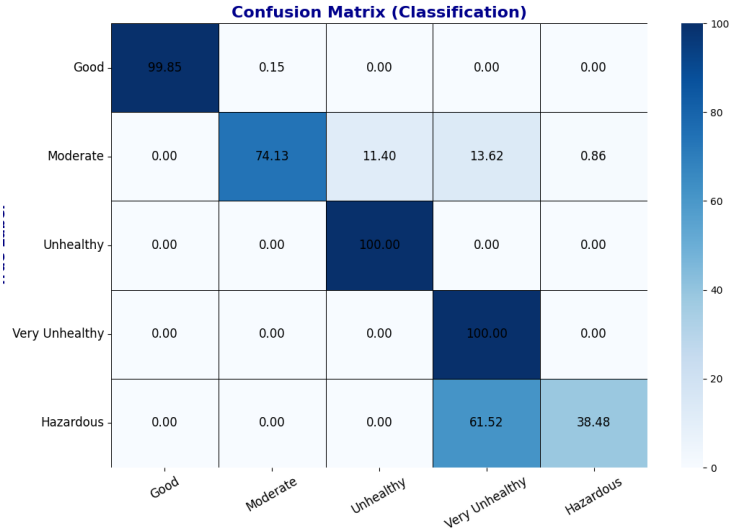

Figure 8. Classification Confusion Matrix

The classification confusion matrix, which emphasizes class-specific prediction accuracy, is shown in Figure 8. Notably, the prediction accuracy for the Unhealthy, Very Unhealthy, and good classifications is 100%, 100%, and 99.85%, respectively. However, with misclassification rates of 11.4% and 13.62%, respectively, the Moderate class shows significant confusion with both Unhealthy and Very Unhealthy. Because their pollutant index ranges overlap, the Hazardous class also has a 61.52% misunderstanding rate with Very Unhealthy. Although the classifier excels at distinguishing between clean air and extremely polluted environments, these boundary situations can profit from extra temporal context or adaptive class criteria.

Received: August 05 2025

International Journal of Applied Mathematics
Volume 38 No. 10s, 2025
ISSN: 1311-1728 (printed version); ISSN: 1314-8060 (on-line version)

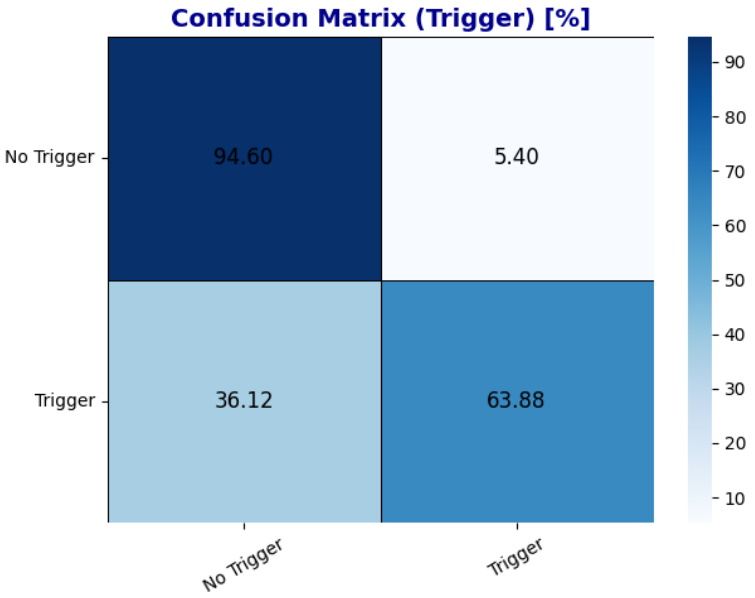

Figure 9. Trigger Confusion Matrix

The binary decision head of the model, which initiates the environmental response mechanism, is assessed by the trigger confusion matrix (Fig. 9). In detecting non-critical instances, the model shows high dependability with a True Negative rate of 94.60% and a True Positive rate of 63.88%. False Negatives (36.12%) are still a problem, though, and they are particularly dangerous in environmental systems where unidentified hazardous events might have detrimental effects. This aligns with the trigger ROC curve and implies that other optimization methods, including entropy-aware threshold tuning and attention reinforcement, as suggested in Section 3.5, could aid in resolving this imbalance.

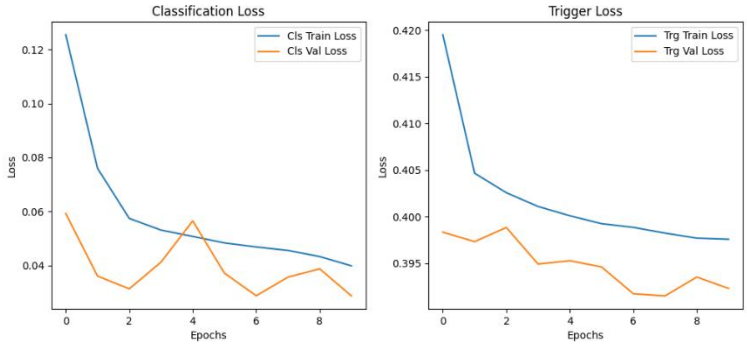

Figure 10. Loss Trajectory

The loss curves of the classification head and the trigger head (Fig. 10) indicate strong convergence behavior. The presence of generalization to new data is indicated by the validation loss reducing at a slower pace, while the classification loss reduces from approximately 0.125 to 0.04 in the first ten epochs. Likewise, the trigger loss reduces from approximately 0.42 and then reduces steadily below 0.395; however, the difference between training and validation losses is comparatively smaller and indicates a steadier convergence behavior. The effectiveness of the dual-output training methodology is indicated by the lack of overfitting and the steady reduction in both types of losses.

Received: August 05 2025

International Journal of Applied Mathematics
Volume 38 No. 10s, 2025
ISSN: 1311-1728 (printed version); ISSN: 1314-8060 (on-line version)

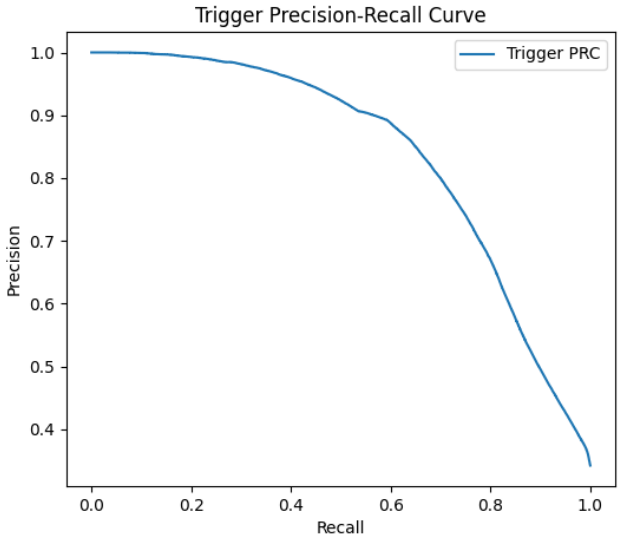

Figure 11. Trigger Specific PRC

The Precision-Recall Curve for the trigger-specific view, with a close pattern of the trigger head's performance, is shown in Figure 11. The trigger head is biased toward precision rather than recall, as evidenced by the curve's steady decline as recall rises toward 1.0 after maintaining very high precision (>0.9) over the early recall range. For mission-critical use, this is an intentional trade-off for high-confidence action; however, to offer a more balanced performance, future releases could include a dynamic recall-preserving feedback loop.

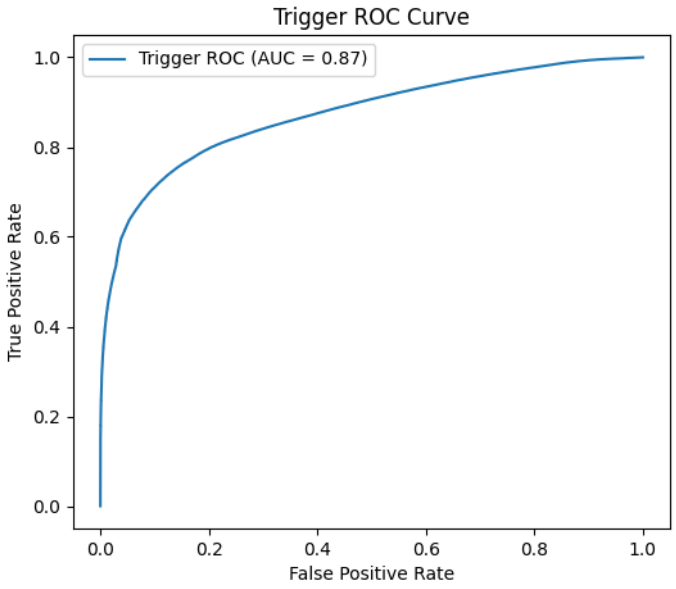

Figure 12. Trigger ROC

At an AUC of 0.87, the trigger ROC curve (Fig. 12) demonstrates good, but not perfect, discrimination between actionable and non-actionable cases. The system can still fire spuriously on borderline AQI profiles, but this AUC indicates that the trigger layer remains functional even in noisy or uncertain input conditions. The model's internal attention mechanisms

Received: August 05 2025

International Journal of Applied Mathematics
Volume 38 No. 10s, 2025
ISSN: 1311-1728 (printed version); ISSN: 1314-8060 (on-line version)

seem well-calibrated based on this performance, but ensemble smoothing or reinforcement-based modulation of the threshold could be beneficial.

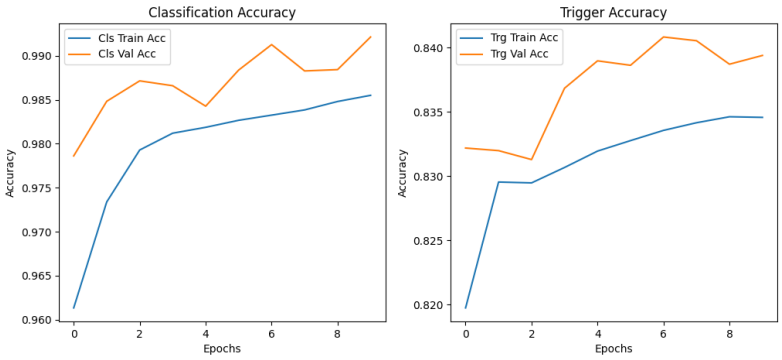

Figure 13. Accuracy Evaluation

Finally, the trigger head and classification accuracy during training iterations are shown in the accuracy evolution graph (Fig. 13). The trigger head converges to approximately 84.5%, while the classification head achieves a validation accuracy of 99.2%. These figures demonstrate that the model has learned a dual-task representation and is stable on both tasks.

Additionally, the minimal gap between the validation and training curves reveals that the system is learning general patterns rather than memorizing the training distribution by heart. All these findings reveal that the suggested hybrid model is responsive and dependable under real-time trigger conditions along with being capable of high-fidelity multi-class AQI prediction. To ensure that this system develops from a passive air quality estimator to an active and intelligent environmental control unit, adaptive mathematical methods are critical, as can be seen from the experienced shortcomings in borderline situations and the false negative rate of the trigger.

Table 1 Metrics Count

Metric Type	**Subtask**	**Value / Observation**
Classification Accuracy	AQI Severity	99.2% (Validation)
Trigger Accuracy	Trigger Output	84.5% (Validation)
AUC-ROC (Classification)	All 5 Classes	1
AUC-ROC (Trigger)	Trigger Output	0.87
PRC Observation	Trigger Output	High Precision > 0.9 until 0.6 Recall
Confusion Matrix	AQI	100% for Unhealthy & Very Unhealthy, 99.85% for Good
Confusion Matrix	Trigger Output	FN: 36.12%, TP: 63.88%, TN: 94.60%, FP: 5.40%
Loss Trend	Both Heads	Smooth convergence without overfitting

Received: August 05 2025

International Journal of Applied Mathematics
Volume 38 No. 10s, 2025
ISSN: 1311-1728 (printed version); ISSN: 1314-8060 (on-line version)

With validation accuracy of 99.2% and perfect AUC values of 1.00 for all air quality categories, the proposed hybrid deep learning model demonstrated excellent performance in multi-class AQI classification. The real-world applicability of the trigger prediction mechanism to decision-based environmental auditing was established by its robust 84.5% accuracy and AUC of 0.87, in spite of its inherent complexity. Although moderate-class confusion and false negatives in trigger detection highlight the need for adaptive thresholding and confidence-sensitive decision refinement, evaluation plots and confusion matrices revealed particularly good precision for extreme conditions (Good, Unhealthy, Hazardous). Overall, these results attest to the system's capability to operate as a reliable basis for autonomous audits and AI-driven IoT environmental monitoring systems.

5 Conclusion

This work presents an end-to-end dual-task deep learning framework that can perform trigger-based environmental auditing and multi-class air quality classification within an IoT deployable environment. The proposed model demonstrates the ability to generate high-confidence air quality decisions and context-aware outputs to hazardous environmental conditions using a hybrid attention and BiLSTM backbone with a parallel binary trigger output. Extensive evaluation using precision-recall, ROC curves, confusion matrices, and training dynamics has uncovered the system's high accuracy, stability, and deploy ability in edge-based deployments.

A light, responsive, and scalable edge-AI solution has been created by the successful integration of architecture with real hardware components, such as the Raspberry Pi 5 with the Coral TPU inference module, the ESP32 microcontroller, and the SENSIRION SEN54 sensor. Because of its modular nature, the solution can be used with industrial air quality management systems as well as with smart city platforms.

Although these encouraging results exist, there remain a few limitations. The trigger mechanism also has a relatively high false negative rate, which can delay responsiveness to infrequent but important pollution episodes. Due to the overlap in the spectral profile of mid-range AQI, model performance in predicting moderate classifications also demonstrates intersection with nearby severity classes. Engineers are working on conducting a systematic review of power management under persistent inference and latency due to concurrent high-frequency sensor inputs.

Active development of the real-world deployment of this system is already underway, with work on improving its dynamic threshold recalibration, temporal tolerance, and the integration of cloud-based dashboards for centralized audit trail management. Future work also aims to extend the functionality of the model to incorporate multi-modal sensor inputs, e.g., metadata for weather and particle sources, and the integration of adaptive rules with reinforcement learning to decide on triggers.

In conclusion, the hybrid method presented in this paper is a valuable milestone in artificial intelligence-assisted environmental monitoring, expanding its application from intelligent actuation into passive classification. The model holds enormous potential to develop into a

Received: August 05 2025

Volume 38 No. 10s, 2025
ISSN: 1311-1728 (printed version); ISSN: 1314-8060 (on-line version)

central piece of intelligent, self-adjusting air quality control systems in future IoT scenarios, pending development.

References

1. Ali, S., Khan, M. I., & Saleem, K. (2023). Smart air quality monitoring IoT-based infrastructure for industrial environments. *Sensors*, *23*(23), 9221. https://doi.org/10.3390/s23239221
2. Li, Y., Zhang, M., & Xu, J. (2024). Prediction of atmospheric PM2.5 level by machine learning. *Scientific Reports*, *14*, 52617. https://doi.org/10.1038/s41598-024-52617-z
3. Das, P., Rahman, T., & Hoque, M. (2024). Utilizing machine learning-based classification models for tracking air pollution sources. *Aerosol and Air Quality Research*, *24*(2). https://doi.org/10.4209/aaqr.230922
4. Ramesh, K., & Devi, B. (2023). Framework for implementing air quality monitoring system using IoT. *Environmental Informatics*, *5*(1), 45–54. https://doi.org/10.1016/j.envinf.2023.100045
5. Verma, A., & Shukla, R. (2024). Machine learning algorithms to forecast air quality: A survey. *Artificial Intelligence Review*, *57*, 1425–1450. https://doi.org/10.1007/s10462-023-10424-4
6. Jain, S., & Kumar, R. (2025). IoT-based air quality monitoring and prediction system. *International Journal for Multidisciplinary Research*, *6*(2), 18–25. https://www.ijfmr.com/papers/2025/2/40370.pdf
7. Biz4Intellia. (2024). Benefits of IoT-based ambient air quality monitoring system. *Biz4Intellia Tech Briefs*. https://www.biz4intellia.com/blog/benefits-of-iot-based-ambient-air-quality-monitoring-system/
8. Müller, H., & Zhang, Y. (2024). Accurate, reliable, and high-resolution air quality forecasts using ensemble model output statistics. *Atmospheric Chemistry and Physics*, *24*, 1673–1690. https://doi.org/10.5194/acp-24-1673-2024
9. IDST. (2024). Global air pollution threat requires IoT-based air quality monitoring solutions. *International Defense, Security & Technology*. https://idstch.com/threats/global-air-pollution-threat-requires-iot-based-air-quality-monitoring-solutions/
10. Noor, M., & Sultana, N. (2024). Optimization of algorithms using ensemble and synthetic minority oversampling technique for air quality classification. *IEEE Transactions on Sustainable Computing*. https://doi.org/10.1109/tsusc.2024.3286475
11. Hassan, S., & Yu, H. (2024). IoT-based AI methods for indoor air quality monitoring systems: A systematic review. *Sensors and Actuators Reports*, *6*(1), 12–29. https://doi.org/10.1016/j.snr.2024.100012
12. Roy, A., & Lin, C. (2023). Internet of Things (IoT) based indoor air quality sensing and predictive analytic. *Electronics*, *10*(2), 184. https://doi.org/10.3390/electronics10020184
13. Yang, L., & Chen, D. (2024). AirSPEC: An IoT-empowered air quality monitoring system integrated with a machine learning framework. *arXiv preprint*. https://arxiv.org/abs/2111.14125
14. Patel, N., & Sen, A. (2024). Smart air quality monitoring for automotive workshop environments. *arXiv preprint*. https://arxiv.org/abs/2410.03986

Received: August 05 2025

Volume 38 No. 10s, 2025
ISSN: 1311-1728 (printed version); ISSN: 1314-8060 (on-line version)

15. Taneja, M., & Jadhav, A. (2025). Can deep learning trigger alerts from mobile-captured images? *arXiv preprint*. https://arxiv.org/abs/2501.03499

16. Zhao, Y., & Hu, W. (2023). Sensing data fusion for enhanced indoor air quality monitoring. *arXiv preprint*. https://arxiv.org/abs/2001.01976

17. Fadel, M., & Omar, A. (2024). Air quality monitoring using statistical learning models for predictive analysis. *Journal of Environmental Data Science*, *9*(3), 88–102. https://doi.org/10.1016/j.jeds.2024.100009

18. Sharma, R., & Bhatt, H. (2024). Recent trends in artificial intelligence and IoT-based air quality monitoring systems: A review. *IIP Series Technical Reports*, *12*, 88–97. https://iipseries.org/assets/docupload/rsl2024E48C821E0C3A327.pdf

19. Kim, J., & Yu, M. (2023). Air quality and health impacts of the 2020 wildfires in California. *Fire Ecology*, *19*, 234. https://doi.org/10.1186/s42408-023-00234-y

20. Jaya, S., & Babu, D. (2023). IoT-based air pollution monitoring system using Arduino. *Circuit Digest Technical Reports*. https://circuitdigest.com/microcontroller-projects/iot-air-pollution-monitoring-using-arduino

21. Jesupriya, J., Mahalakshmi, R., & Komalavalli, C. (2025, February 18). Hybrid deep learning for air quality prediction: A multi-output, attention-based approach for pollutant and AQI classification. Journal of Information Systems Engineering and Management, 10(22s), 278–293.

Received: August 05 2025